Available online at www.sciencedirect.com
ScienceDirect
Journal of Controlled Release 118 (2007) 27–37
journal of controlled release
www.elsevier.com/locate/jconrel

Biodegradable *in situ* gelling system for subcutaneous administration of ellagic acid and ellagic acid loaded nanoparticles: Evaluation of their antioxidant potential against cyclosporine induced nephrotoxicity in rats

G. Sharma [a,b], J.L. Italia [a,b], K. Sonaje [a], K. Tikoo [c], M.N.V. Ravi Kumar [a,b,*]

[a] *Department of Pharmaceutics, National Institute of Pharmaceutical Education and Research (NIPER), S.A.S. Nagar, Mohali, Punjab, 1600 62, India*
[b] *Centre for Pharmaceutical Nanotechnology, National Institute of Pharmaceutical Education and Research (NIPER), S.A.S. Nagar, Mohali, Punjab, 1600 62, India*
[c] *Department of Pharmacology and Toxicology, National Institute of Pharmaceutical Education and Research (NIPER), S.A.S. Nagar, Mohali, Punjab, 1600 62, India*

Received 11 September 2006; accepted 25 November 2006
Available online 6 December 2006

Abstract

Ellagic acid (EA) is a potent antioxidant marketed as a nutritional supplement. Its pharmacological activity has been reported in wide variety of disease models; however its use has been limited owing to its poor biopharmaceutical properties, thereby poor bioavailability. The objective of the current study was to develop chitosan-glycerol phosphate (C-GP) *in situ* gelling system for sustained delivery of ellagic acid (EA) via subcutaneous route. EA was incorporated in the system employing propylene glycol (PG) and triethanolamine (TEA) as co-solvents; on the other hand EA loaded PLGA nanoparticles (np) were dispersed in the gelling system using water. These *in situ* gelling systems were thoroughly characterized for mechanical, rheological and swelling properties. These systems are liquid at room temperature and gels at 37 °C. The EA C-GP system showed an initial burst release *in vitro* with about 85% drug released in 12 h followed by a steady release till 160 h, on the other hand EA nanoparticles entrapped in the C-GP system displayed sustained release till 360 h. The histopathological analysis indicates the absence of inflammation on administration, suggesting that these formulations are safe during the studied period. Furthermore, the antioxidant potential of EA C-GP and EA np C-GP gels has been evaluated against cyclosporine induced nephrotoxicity in rats. The data indicates that formulations were effective against cyclosporine induced nephrotoxicity, where the EA C-GP gels showed activity at 10 times lower dose and the EA np C-GP gels at 150 times lower dose when compared to orally given EA. Formulating nanoparticles of EA and incorporating them in C-GP system results in 15 times lowering of dose in comparison EA C-GP gels which is quite significant. Together, these results indicate that the bioavailability of ellagic acid can be improved by subcutaneous formulations administered as simple EA or EA nps.

Keywords: Antioxidants; Biodegradable; Chitosan; Ellagic acid; Free radicals; In situ; Nephrotoxicity

1. Introduction

With developments in biochemistry and medicine, it is now well established that free radicals play a significant role in the etiology and pathogenesis of many human diseases [1–4] like neurodegenerative disorders, cardiovascular complications, diabetes, hypertension, cancer and ageing. The relationship between free radicals and disease is explained by oxidative stress which is defined as an imbalance between oxidants and antioxidants in favor of the oxidants, potentially leading to cell damage [5,6] under the influence of adverse physicochemical environment or pathological agents. Antioxidants are substances that neutralize free radicals by delaying or inhibiting oxidation of substrate on which free radicals attack [7,8]. Their protective efficacy depends on the type of reactive oxygen species (ROS) that is generated, the place of generation and the severity of damage [9,10]. The role of dietary antioxidants [11] as prophylactics and therapeutic agents in different diseases is well

* Corresponding author. Department of Pharmaceutics, and Centre for Pharmaceutical Nanotechnology, National Institute of Pharmaceutical Education and Research (NIPER), S.A.S. Nagar, Mohali, Punjab, 1600 62, India. Tel.: +91 172 2214683 89x2055; fax: +91 172 2214692.
E-mail addresses: mnvrkumar@niper.ac.in, mnvrkumar@yahoo.com (M.N.V. Ravi Kumar).

0168-3659/$ - see front matter © 2006 Elsevier B.V. All rights reserved.
doi:10.1016/j.jconrel.2006.11.026

established [12]. Certain phytonutrients have shown to posses multiple pharmacological effects including antioxidant, anti-inflammatory and anticancer properties and hence can be used in patients with multiple diseases.

Ellagic acid (EA) is one such polyphenolic phytonutrient found in wide varieties of berries and nuts, which has already proven its antioxidant potential both *in vitro* [13] and *in vivo* [14]. Experimental evidences using animal models reflect that orally administered EA is poorly absorbed and rapidly eliminated from the body which limits its potential as a systemic antioxidant due to its inability to attain required tissue concentrations [15,16]. The low oral bioavailability of EA is attributed to its low aqueous solubility, metabolism in GIT [17], irreversible binding to cellular DNA and proteins and first pass effect. There are a number of EA extracts on the market especially of red raspberry and the extracts are available in capsule, powder, or liquid form. A "safe and effective" oral dose of EA or salts or esters thereof depends on the therapeutic application and extent of the disease. However, there is no formulation available that can deliver therapeutically adequate dose due to poor bioavailability issues of EA, attributed to its biopharmaceutical and pharmacokinetic properties. Poorly water soluble drug compounds are often difficult to process into dosage forms that afford adequate oral bioavailability for clinical studies and commercialization and EA is poorly soluble compound (water solubility $\simeq$9.7 μg/ml) [18]. Hence there is a strong need to deliver this molecule by unconventional means which can circumvent biopharmaceutical and pharmacokinetic issues related with EA without compromising its therapeutic potential.

In situ gelling systems are gaining importance in drug delivery nowadays [19], due to the advantages these systems possess over the conventional parenteral formulations, which includes: ease in administration, localized delivery, sustained delivery over a long period of time, dose reduction, ease of fabrication, ability to deliver poorly water soluble drugs and increased patient compliance. In the past few years, an increasing number of *in situ* gelling systems have been reported in literature for biomedical applications, drug delivery, cell encapsulation and tissue repair. These systems are liquid at room temperature but undergo sol–gel transitions when temperature is increased. Out of several polymers like PNIPAM, Poloxamer, PMMA; which have been investigated for fabrication of *in situ* gelling systems; chitosan (CS) is the most extensively studied polymer and is biocompatible and biodegradable amino polysaccharide that has been extensively used in controlled drug delivery [20]. Recently Chenite et al. [21] developed a novel *in situ* gelling system for subcutaneous administration, by neutralizing chitosan solution with glycerol phosphate. The system is liquid at room temperature but forms a gel at physiological temperature and was examined for delivery of poorly water soluble drugs like paclitaxel and camptothecin which suffer from poor bioavailability. Therefore, the objective of the present study was to design and characterize chitosan-glycerol phosphate *in situ* gelling system for delivery of EA and EA acid loaded nanoparticles for subcutaneous administration, aiming to enhance its delivery prospects.

2. Materials and methods

2.1. Materials

Chitosan (medium mol wt, medium viscosity grade) having a deacetylation degree of 91% was obtained from Cochin (India). GP (cell culture grade) was purchased from Sigma (US). EA was purchased from Fluka (US). The commercial formulation of Cyclosporine (CyA) Sandimmune Neoral® Novartis was purchased from a local pharmacy store. Poly (lactide-co-glycolide) (PLGA) (Resomer RG 50:50 H; inherent viscosity 0.45 dl/g, mol wt 35 kDa–45 kDa) were gift samples from Boehringer Ingelheim (Ingelheim, Germany). Didodecyldimethylammonium bromide (DMAB) was purchased from Aldrich (St. Louis, MO, USA). Ethyl acetate (AR grade) and acetonitrile (ACN; HPLC grade) were purchased from Rankem Fine Chemicals (New Delhi, India). Double distilled water was prepared in house and was used to prepare the aqueous solutions. All products were used as received. All other chemicals were of reagent grade.

2.2. Preparation of blank C-GP gels

Blank C-GP *in situ* gelling system was prepared with slight modifications from the reported method [21]. Briefly, 100 mg CS (DD=91%) was dissolved in 4.5 ml (0.1 N) HCl and the solution was stirred vigorously at 1100 rpm at room temperature for 2 h (or till solution was clear). The pH of the resulting solution was checked. CS solution was chilled to a temperature of 4–5 °C. GP (280 mg) was dissolved in 0.5 ml of distilled water maintained at 4–5 °C and was subsequently added to chilled chitosan solution in a controlled manner. The resulting C-GP mixture was stirred at 2000 rpm for 5 min and the final solution contained 2% (w/v) of CS and 5.6% (w/v) GP. The gelling ability of this preparation was checked by incubating 200 μl at 37 °C.

2.3. Effect of GP concentration on gelling time

GP, in four different concentrations (560 mg/ml, 660 mg/ml, 760 mg/ml and 1000 mg/ml) was used to optimize gelling time of 200 μl of C-GP solution keeping gelling temperature as 37 °C. The effect of GP on the pH of resulting C-GP solution was also evaluated.

2.4. Preparation of EA loaded C-GP gels

EA showed poor solubility in maximum number of available solvents and this hindered its loading in the C-GP gel. Different solvents, co-solvents and wetting agents were screened to load EA in C-GP gel. DMSO, PG, NMP, NMP+PG, TEA, 1% TEA in water, ME and TW80 were employed for this purpose. CS solutions were prepared as mentioned earlier and required amounts of solvents/wetting agents were added in clear CS solutions and stirred at 1100 rpm for 30 min. 50 mg of EA was added in each followed by stirring for 2 h till a homogeneous suspension/dispersion of EA was obtained. The solutions were

chilled to 4–5 °C with stirring and chilled GP solution was then added to each and the solutions were stirred for the next 5 min at 2000 rpm. 200 μl of solution was kept for gelling at 37 °C and their gelling time was recorded. After selection of appropriate solvents/wetting agents, the effect of drug loading on the gelling time was also evaluated. Drug content uniformity was investigated by homogenizing fresh gel samples (200 μl) in methanol–phosphate buffer pH 6.6 1:1 (v/v) mixture followed by analysis using UV (λ_{max}=274 nm).

2.5. Loading EA nanoparticles in C-GP gel

EA loaded PLGA nanoparticles were prepared by adopting modified Emulsification–diffusion–evaporation method developed in our lab [22]. The encapsulation efficiency and purification were performed as reported earlier [18,22,23]. CS solution were prepared and chilled in the same manner as stated before and EA loaded PLGA nanoparticles (drug content 1.0 mg/50 mg of nanoparticles) dispersed in different volumes of water were added in the CS solution without using co-solvents and stirred for the next 5 min. Chilled GP solution was then added to each and the solutions were stirred for the next 5 min at 2000 rpm. 200 μl of solution was kept for gelling at 37 °C and their gelling time was recorded.

2.6. Characterization using FTIR

The interactions which led to the formation of C-GP gel were investigated using FTIR (Perkin Elmer, USA). Both blank and EA loaded gels were dried overnight at 55 °C in vacuum oven to remove water and grinded with KBr in equal proportion to form pellets which were subjected to analysis and CS, EA served as controls.

2.7. Swelling studies

Gravimetric method was adopted in characterizing pH dependent swelling of C-GP gels. Freshly prepared gels in the form of discs (200 μl each) were placed in phosphate buffers at pH 1.2 and 6.6 at 37 °C. Changes in weight of gels as a function of time after blotting the surface water with soft tissue paper was recorded and subsequently swelling ratios were calculated from the standard formulae.

$$\text{Swellingratio} = [W_t/W_0].$$

W_t=Weight of swollen gel at time t and W_0=Initial weight of gel. Swelling kinetics was defined by the change of swelling ratio versus time.

2.8. Mechanical properties

The mechanical properties of all gel formulations were examined using a Stable Micro System texture analyzer (Model TAXT2i) in texture profile analysis (TPA) mode. Formulations were transferred into 5 ml beaker to a fixed height, taking care to avoid the introduction of air into the sample. In TPA mode the analytical probe (10 mm diameter ebonite cylinder) compressed into each sample at a defined rate (1 mm/s) to a depth of 15 mm and then retraced its path back. The acquisition parameters were 5 mm/s pre-speed, 1 mm/s test speed, 10 mm/s post-speed with an acquisition rate of 50 points/s and 5 kg load cell. The resulting profiles were analyzed using Texture Expert, Version 1.22 (Stable Micro Systems, Surrey, UK). The profiles were analyzed for firmness, cohesiveness and consistency of all gel formulations. Using modified Water's equation qualitative change in the Young's modulus was also determined to predict changes in mechanical properties of the system undergoing sol–gel transition.

2.9. Rheological measurements

Rheological investigations were carried out using Brookfield's Rheometer model DVIII+ using Rheocal software with SC4 21 spindle in cup bob geometry. Freshly prepared blank C-GP solution was first transferred in the cup which was maintained at 2 °C. The solution was allowed to stabilize at 2 °C for 10 min and viscosity and rheogram was obtained by applying differential rpm loop. Temperature was then changed to 16 °C and system was again allowed to stabilize at 16 °C for the next 10 min and again viscosity and rheogram was obtained applying differential rpm loop. This procedure was followed for 25 °C and 37 °C. For EA loaded and EA nanoparticles loaded gels, the fresh solutions were allowed to stabilize at 37 °C and applying differential rpm loop method viscosities and rheograms were obtained.

2.10. In vitro release studies

EA and EA np loaded gels were analyzed for *in vitro* release. Freshly prepared EA loaded (1 mg EA in 200 μl of C-GP gel) and EA np loaded (nanoparticles equivalent to 1 mg EA in 200 μl of C-GP gel) C-GP solutions were transferred into dialysis membrane having a molecular weight cut off 12,000 Daltons. The dialysis membranes were then suspended in 20 ml phosphate buffer pH 6.6 (pre-warmed to 37 °C) which was selected as the release media to mimic pH of subcutaneous tissue and was prepared as per specifications of British compendia. The solutions were allowed to gel inside the dialysis membrane in contact with release media at 37 °C. 20 μl of 0.1% sodium azide was added to provide antifungal conditions. Lysozyme (2 mg/100 ml) was added in the release media to further mimic subcutaneous tissue environment. The test was conducted in a shaker bath maintained at 37 °C with 100 rpm. At predetermined time intervals complete release medium was sampled and replaced with 20 ml of fresh medium. All dilutions were prepared in phosphate buffer 6.6 and were analyzed by UV (λ_{max}=274 nm in phosphate buffer pH 6.6) for EA loaded gels and by HPLC (with UV detector) for EA np loaded gels.

2.11. Histopathological studies

For assessing biocompatibility of C-GP gel formulations, histopathological studies were carried out using adult male

Sprague Dawley rats (weighing 250–300 g). The study was done following the guidelines for care and use of experimental animals as laid down by the Institutional Animal Ethics Committee (IAEC) of NIPER. Animals were divided into six groups (nine rats in each group). Group 1 was the control, group 2 received PG containing blank gels, group 3 received TEA containing blank gels, group 4 received EA loaded gels formulated employing PG, group 5 received EA loaded gels formulated using TEA and group 6 was given EA np loaded gel formulations. Freshly prepared blanks, EA loaded, EA nanoparticles loaded C-GP formulations were administered subcutaneously on the dorsal side over a period of 15–20 s by using 22 gauze needles without anesthesia. The dose administered was 200 µl containing 15 mg of free EA and nanoparticles equivalent to 1 mg of EA for nanoparticle formulation along with blank gels containing PG and TEA separately. The animals were fed with regular diet and water ad libitum and were exposed to normal light and dark cycles. First sampling was done on the next day, second sampling was done on the 5th day and the final on the 15th day from the day of administration of gels and on each of these time points three animals from each group were sacrificed and analyzed for changes in the subcutaneous tissue. The animals were sacrificed by cervical dislocation and their intact skin along with subcutaneous tissue was excised. The freshly excised tissues were stored in 10% formal saline till analysis. The sections were made using microtome. Thin sections of the tissue embedded in wax were finally stained with hematoxylin and eosin. The sections were mounted on slides using DPX and observed under high magnification (100×/450×/630×) light microscope to check histopathological changes.

2.12. In vivo analysis of formulations

For evaluating antioxidant potential of EA and EA nanoparticles loaded C-GP gel formulations, nephrotoxicity studies (Table 1) were carried out using adult male Sprague Dawley rats weighing 250–300 g (IAEC guidelines of NIPER were followed). Animals were divided into six groups at $n=3$ (three animals per group). Treatment was commenced from day one. All groups except control (Group 1) received daily dose of 15 mg/kg body weight. CyA orally in the form of Sandimmune Neoral® (marketed micro-emulsion of cyclosporine) for 30 days resulting in CyA induced nephrotoxicity. The toxicity was monitored by blood urea nitrogen concentration (BUN), serum creatinine and MDA levels in plasma and kidneys. Group 2 received only Neoral dosing for the studied period and in case of EA treated groups; EA susp group (Group 3) received daily 50 mg/kg body weight of EA as a suspension in 0.5% w/v CMC vehicle along with daily dose of CyA. Blank gel group (Group 4) received 200 µl of blank C-GP sol subcutaneously on every 10th day. EA gel group (Group 5) received 50 mg/kg body weight of EA loaded in 200 µl of C-GP sol, prepared using PG on every 10th day, whereas EA np gel group (Group 6) received nanoparticles equivalent to 1 mg of EA suspended in 200 µl of

Table 1
Nephrotoxicity study plan

Groups in serial order	Neoral dosing (15 mg/kg body weight)	Frequency of administration of EA and EA gel formulations: at dose of 50 mg/kg body weight	Total dose of EA administered over the study period (mg)
Control	–	–	–
Neoral	✔	–	–
EA Susp	✔	Daily	450
Blank gel (s.c.)	✔	Every 10th day	–
EA gel (s.c.)	✔	Every 10th day	45
EA np gel (s.c.)	✔	Every 10th day	3

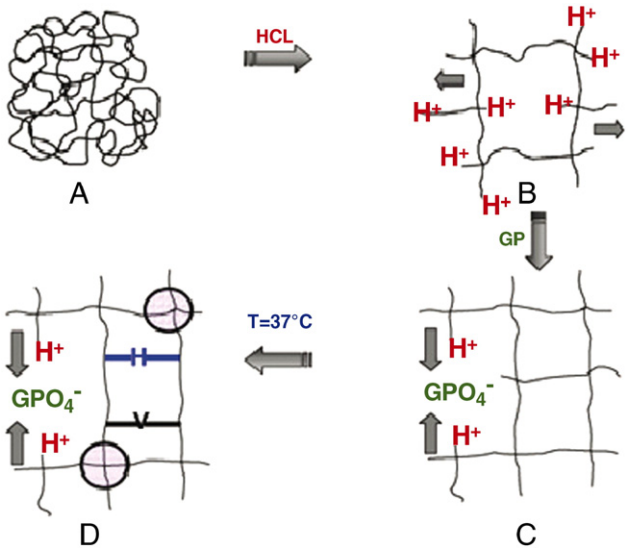

Fig. 1. Schematic representation of expected gelling mechanism in C-GP system: (A) CS in native state; (B) solubilization of CS in HCl; on adding HCl, the amino groups in CS get protonated and thereby develop positive charges which leads to the electrostatic repulsion between CS chains and this keeps CS chains dispersed in acidic solution. (C) Addition of GP; GP causes development of physical cross linking by bridging effect of negative charged phosphate group on protonated amino groups. (D) Gelling; increasing temperatures to 37 °C leads to formation of physical junction zones (circles) which bring CS chains closer and on coming closer, CS chains develop van der Waals attraction (V), hydrogen bonding (H) and hydrophobic interactions which eventually lead to gelation.

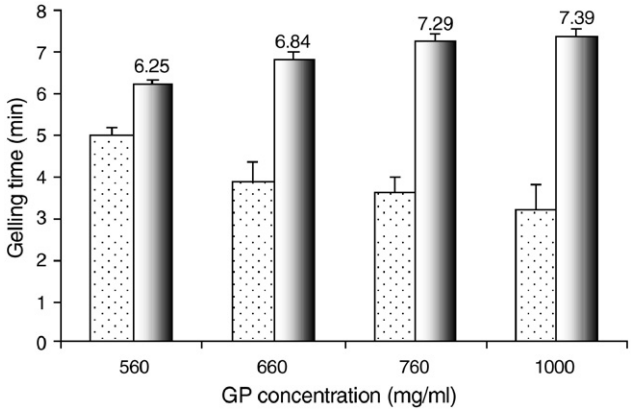

Fig. 2. Influence of GP concentration on gelling time and pH of C-GP solutions. Dotted bars represent gelling time of C-GP solution while solid bars represent pH of the respective C-GP solutions. (Data represents Mean±SD) $n=3$.

Table 2
Solvent screening for loading EA in C-GP solution

Co-solvent	Quantity used	Gelling at 37 °C	Gelling time (min)
Methanol	100 µl	No	–
DMSO	20 µl	No	–
NMP	20 µl	No	–
PEG 400	100 µl	No	–
NMP+PG	20 µl+20 µl	Yes	10
PG	20 µl	Yes	07
TEA	20 µL	No (precipitation)	
1% TEA in water	1 ml	Yes	06
1% Tween 80 in water	1 ml	Yes	05

C-GP sol, on every 10th day. On the 31st day, the study was terminated and the animals were sacrificed by decapitation and blood was collected in heparinized centrifuge tubes. The blood samples were centrifuged and plasma was collected. The MDA levels were estimated immediately, whereas remaining plasma was stored at −20 °C for analysis of BUN concentration and creatinine using standard diagnostic kits. A middle abdominal incision was performed and both kidneys were removed. The left kidney was stored in 10% formalin solution for histopathological analysis and the right kidney was thoroughly washed with ice cold phosphate buffer, weighed, minced and homogenized in phosphate buffer pH 7.4 (volume equivalent to five times the weight of kidney). Homogenates were centrifuged at 10 °C and MDA and total protein were estimated in supernatant.

2.13. Statistics

Statistical difference between treatment groups was evaluated via one-way analysis of variance (ANOVA) using Sigma Stat 2.0 software (Jindal Scientific); a value of $p<0.05$ was considered significant.

3. Results and discussions

3.1. Preparation of blank C-GP gels

Blank C-GP gels were prepared with slight modifications from the reported method of Chenite et al. [21]. The solubility of CS in acid is explained by protonation phenomenon where the free amino groups present in CS are protonated and this leads to development of electrostatic repulsion between CS chains. Moreover, pH of solution increases from 1.23 to 5.3 and when GP is added, the negatively charged phosphate groups from GP neutralize positively charged amino groups on CS thereby decreasing electrostatic repulsions due to which CS chains come closer and develop hydrogen bonds, hydrophobic interaction and van der Waals attraction (Fig. 1). Glycerol moieties from GP have additional water structuring effect. When temperature was raised to 37 °C there was development of physical junction zones between CS chains which leads to complete gelation of C-GP solution. The neutral character of C-GP gel was evident from their final pH, which was around 6.8 to 7.2. The gelation was monitored using vial inversion method. The gelling time was recorded for 200 µl of the C-GP solution.

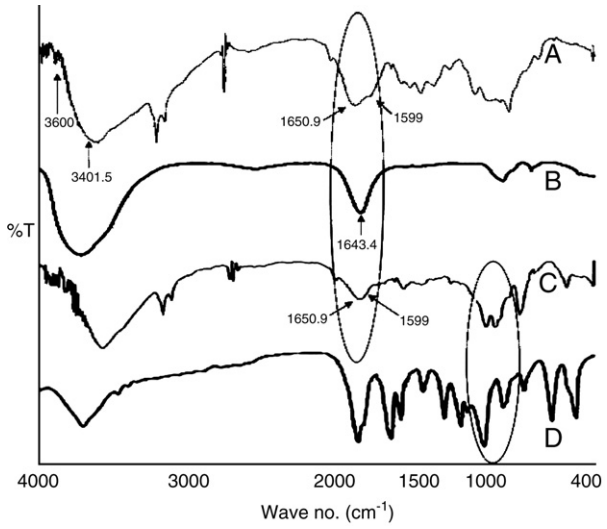

Fig. 4. FTIR overlay of blank chitosan (CS), blank C-GP gel, EA loaded C-GP gel and EA.

3.2. Effect of GP concentration on gelling time

Since the gelation mechanism involved an interaction of GP with protonated CS, the concentration of GP was investigated as

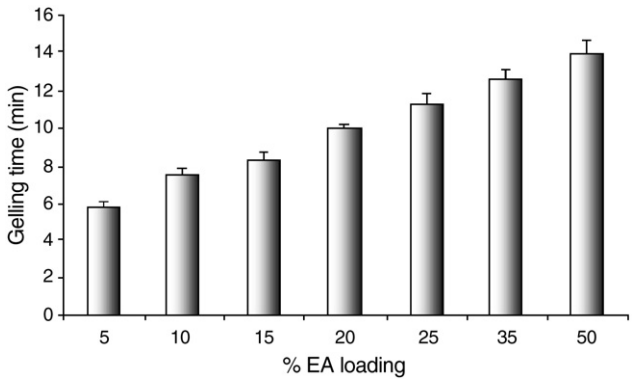

Fig. 3. Influence of EA loading on gelling time of C-GP solutions (Data represents Mean±SD) $n=3$.

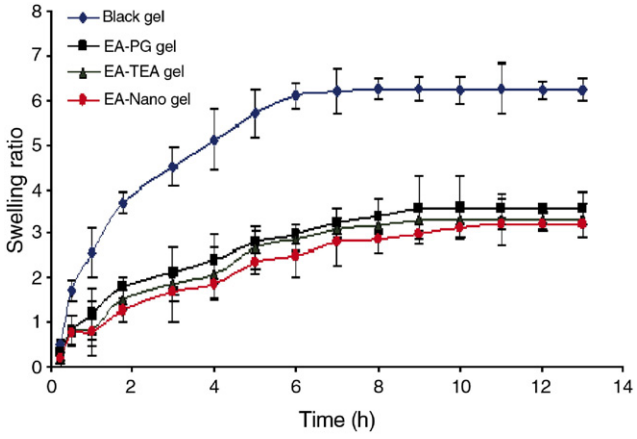

Fig. 5. Swelling profile of different gel formulations at pH 1.2 (Data represents Mean±SD) $n=3$.

one of the factors that affected gelation. Different concentrations of GP which were added to same concentration of CS in 0.1 N HCl. The results clearly showed that with increase concentration of GP for same concentration of CS, gelling time reduced (Fig. 2) as high GP concentration caused rapid neutralization of protonated amino groups from CS. Moreover, high GP concentration is also correlated with higher pH of the system at which CS has the tendency to precipitate due to deprotonation of amino groups. Considering the above, 660 mg/ml was selected as the appropriate concentration of GP for optimum gelling time.

3.3. Preparation of EA loaded C-GP gels

Out of various solvents which were screened to load EA in C-GP system (Table 2), PEG 400 solubilized EA in CS solution but it hindered the gelling property of EA loaded C-GP solutions. PG and 1% TEA were selected for dispersing EA in CS solution as they did not alter gelling ability of EA loaded C-GP systems. In addition both PG and TEA are class two solvents as per ICH guidelines and were safe for use in such low concentrations. Tween 80 was also used but in spite of the fact that EA loaded C-GP solutions with Tween 80 had the least gelling time, it was not employed as the gels formed were fragile and difficult to handle. Different drug loadings were carried out and their effect on gelling time was evaluated and results indicated that gelling time increased with increase in drug loading (Fig. 3) which is attributed to increased amount of drug which is interspersed between CS chains separating them from each other; therefore requiring longer time to develop temperature induced physical junction zones.

3.4. Preparation and loading of EA loaded PLGA nanoparticles in C-GP gel

Ellagic acid loaded PLGA nanoparticles were prepared by adopting previously developed method in our laboratory [22,23] and the particles had average size of 148 nm with 43% encapsulation at 5% drug loading. These nanoparticles were then redispersed in water for loading onto C-GP solution. The volume of dispersed nanoparticles was crucial as a large volume addition resulted in failure of gel formation due to dilution of C-GP solution. The process of EA nanoparticles loaded onto C-GP solution was optimized using different volumes of redispersed nanoparticles in 5 ml of C-GP solution which gave different

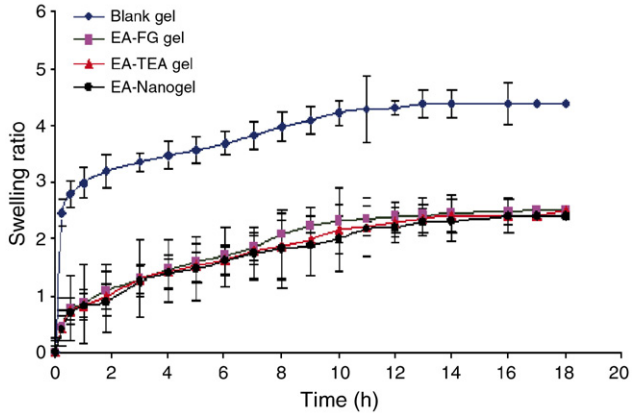

Fig. 6. Swelling profile of different gel formulations at pH 6.6 (Data represents Mean ± SD) $n=3$.

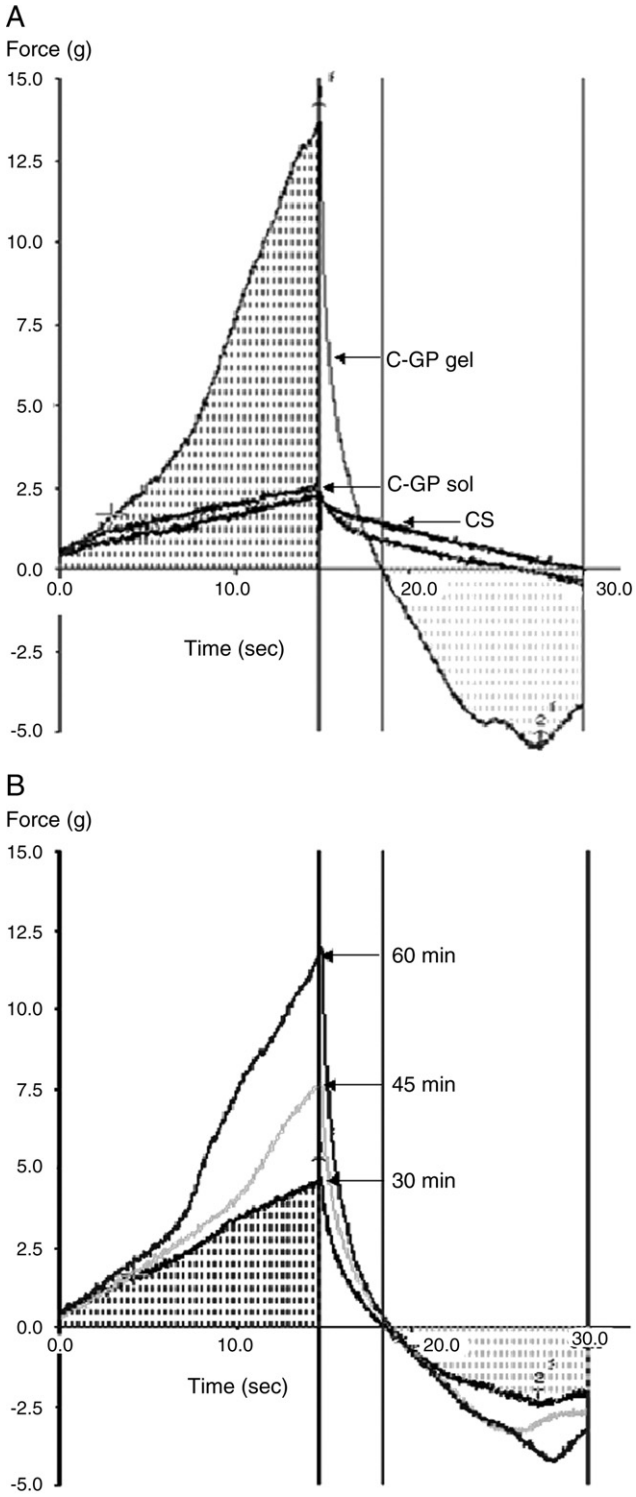

Fig. 7. Texture analysis of gel formulations: (A) texture analysis plots for CS solution, blank sol and blank C-GP gel. (B) Texture analysis plots for blank C-GP gel at different incubation times.

gelling times. On the other hand, addition of vacuum dried nanoparticles resulted in gel formation with minimum gelling time due to least dilution effect on C-GP solution.

3.5. FTIR

The nature of interactions which eventually led to gel formation and the interaction between gel forming components was elucidated by FTIR. Spectra revealed that there was no chemical interaction between the gel forming components (Fig. 4). CS exhibited a broad peak at 3401.5 cm^{-1}, 3600 cm^{-1} which is assigned to the NH and hydrogen bonded O–H stretch vibrational frequencies. C═O stretch of amide bond was observed near 1650.9 cm^{-1}. The peaks around 1550 cm^{-1} were assigned to strong N–H bending of secondary amide. When GP was added in CS solution, the spectra obtained for C-GP gel shows a very slight change in C═O stretch of amide bond which is observed near 1643.4 cm^{-1}, this shows that GP induces formation of possible hydrogen bonds and the interaction of GP with CS is purely physical. The presence of two characteristic peaks of EA (in the range 1300–1050 cm^{-1}) in FTIR of drug loaded gels confirms the absence of any chemical interaction between gel components and EA.

3.6. Swelling studies

Drug loaded C-GP solutions were intended for subcutaneous administration; hence their swelling behavior was evaluated at a pH close to subcutaneous tissue i.e. 6.6. Since CS is a pH sensitive polymer, the degree of swelling is influenced by the pH of the environment. At pH 1.2, the amino groups of chitosan are protonated and this ionization induces electrostatic repulsions between the polymer chains. Moreover, an osmotic pressure in the network is created by the presence of counter ions [24]. The ionization of amine function of CS may lead to the dissociation of possible hydrogen bonds and van der Waals attraction between CS chains and thus leading to relaxation of the macromolecular chains. EA loaded and EA nanoparticle loaded gels showed moderate swelling behavior at pH 1.2 (Fig. 5). This was due to the absence of free interstitial spaces between the CS chains in the three dimensional gel matrices when compared to the blank system. Swelling was greatly reduced at pH 6.6 (reduced to 50% for drug loaded and nanoparticles loaded formulations) due to mild protonation of amino groups of CS at higher pH with concurrent high drug loading (Fig. 6).

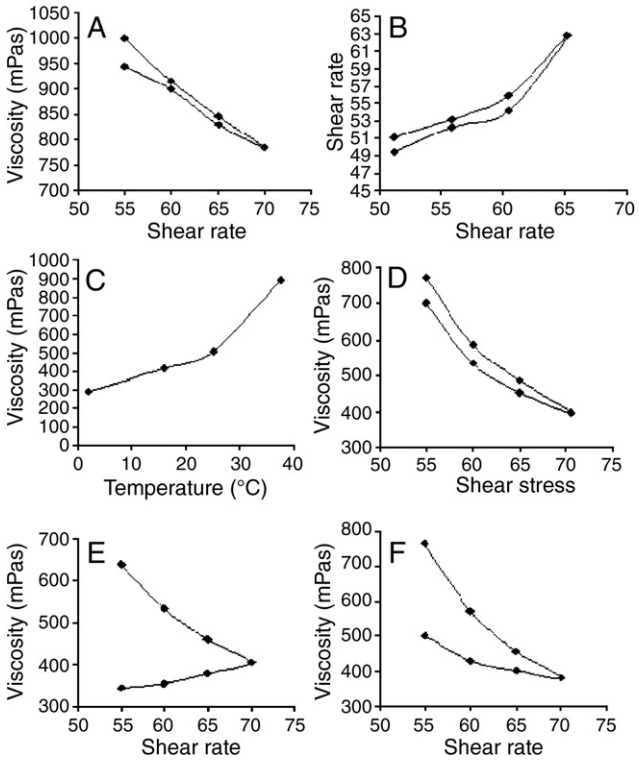

Fig. 8. Rheological profiles of blank C-GP sol and gel. (A) Change in viscosity with shear rate at 37 °C for blank gel. (B) Pseudoplastic curve obtained at 37 °C for blank C-GP gel. (C) Effect of temperature on viscosity of C-GP sol. (D) EA nanoparticle loaded C-GP gel. (E) C-GP EA gel using 1% TEA solution in water. (F) C-GP EA gel using PG.

3.7. Mechanical properties

TA is a penetrometry technique that has been extensively employed in the mechanical characterization of food materials. Recently, it has emerged as a useful technique in the field of pharmaceutical gel characterization [25]. This study permits to evaluate the textural properties of the different formulations in order to obtain information about physical gels structure and to predict sample behaviors under the physiological conditions. When CS solution was subjected to analysis, force vs. time plot obtained, showed that CS solution had typical solution behavior with a certain viscosity value. When C-GP solution at room temperature was analyzed, it showed that there was some phase transformation from solution phase to pre-gel phase or sol phase and this was characterized by increased viscosity and increased

Table 3
Mechanical properties of CS solution, C-GP sol and blank C-GP gel

System	Firmness (max+ve force) g	Cohesiveness (max+ve area) g s	Consistency (max−ve force) g	Recovery (max−ve area) g s	Young's modulus
CS solution	2.3	20.58	0.016	0.001486	0.00064
Sol	2.7	24.66	0.6	0.8065	0.00103
Gel (30 min)	4.8	37.41	2.5	19.6	0.00583
Gel (45 min)	7.8	45.12	3.2	21.11	0.01658
Gel (60 min)	12.0	76.41	4.3	30.25	0.09112
Gel (75 min)	13.8	83.96	5.6	43.15	0.17853

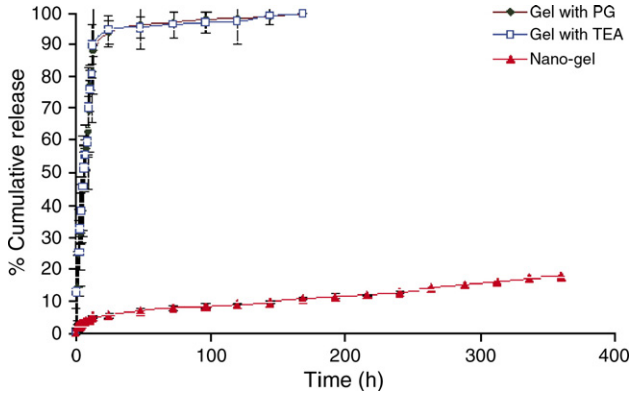

Fig. 9. *In vitro* release from EA loaded (using PG and 1% TEA) and EA nanoparticles loaded gels in phosphate buffer pH 6.6 at 37 °C. (Data represents Mean ± SD) $n=3$.

resistance to penetrating probe for the same penetrating distance (15 mm) by sol system. C-GP solution at 37 °C gave higher values of resistance to penetrating probe and higher viscosity which indicated gelling in the C-GP system. The initiation of gelling was also confirmed by rheology and test-tube inversion method which gave similar results. Penetration/withdrawal profiles of CS solution, C-GP solution at room temperature and blank C-GP gel incubated at 37 °C for 75 min, shows that CS solution has the least firmness, cohesiveness, consistency and adhesiveness while C-GP gel at 37 °C had maximum values (Fig. 7A).

Consistency of a gel is related to its compressibility and hardness. Adhesiveness is the work required to remove the probe from the sample and it is related to the breaking of cohesive bonds. It is dependent on system viscosity but it is also considered a measure of the affinity for non-mucous surface. The lower values of the above mentioned parameters for C-GP sol indicate that it has good syringbility (lower consistency) which is desired, lower viscosity which allows ease in administration to patient and once injected the system attains higher consistency and behaves almost as a solid implant inside the body which further resists any deformation as indicated by viscosity values on long term residence in the subcutaneous tissue. Moreover, higher values of adhesiveness for C-GP gel are desired to maintain an intimate contact with non-mucosal surfaces such as subcutaneous tissue [26]. In addition, TA plots (Fig. 7B) and the qualitative young's modulus (Table 3) obtained using modified Water's equation [27] revealed that there was an increase in elasticity of gels with time. Texture characterization showed that C-GP systems had good mechanical properties both in sol phase as well as in gel phase in terms of firmness, compressibility and adhesiveness.

3.8. Rheological properties

The curved rheograms for C-GP sols and gels resulted from a shearing action on the long chains of chitosan. As the shearing stress was increased, the normally disarranged molecules aligned themselves along their long axis in the direction of flow. This orientation reduced the internal resistance and allowed a greater rate of shear at each successive shearing stress. In addition the water released from the gel resulted in an effective lowering of the concentration and this also added in

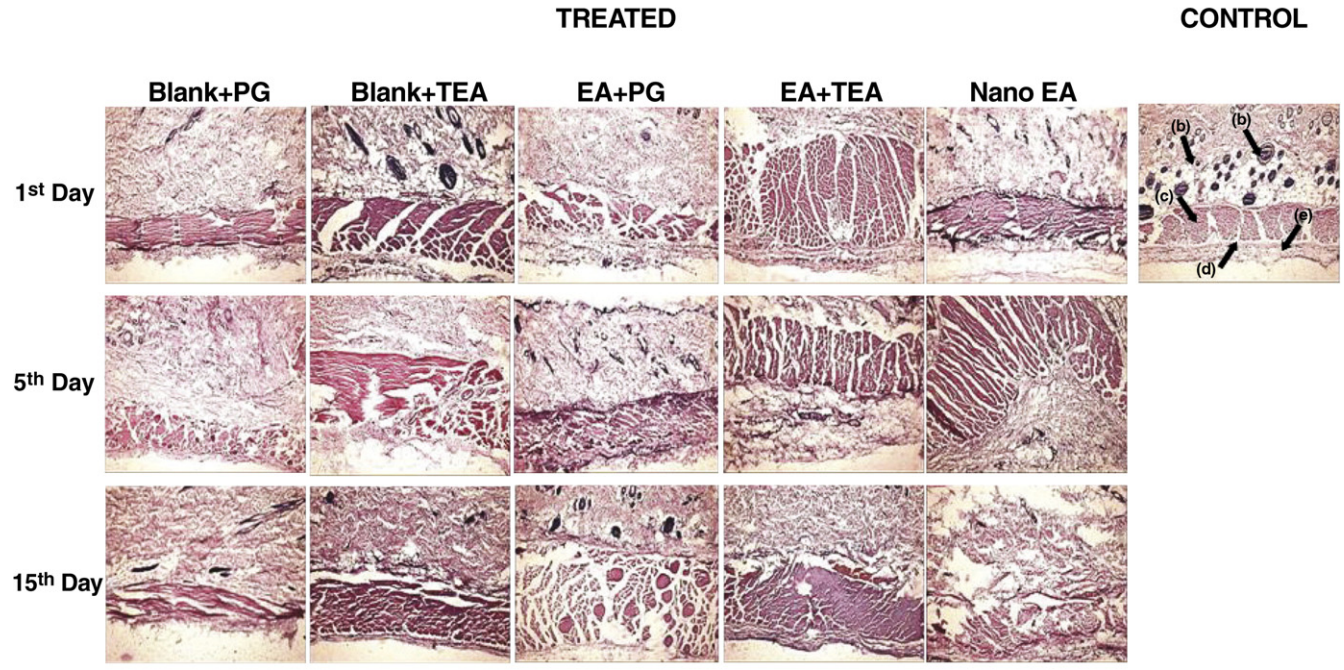

Fig. 10. Microscopic structure of sections of subcutaneous tissue of treated and control groups (a) hair follicles in control group (b) dermis of control (c) muscular layer (d) narrow subcutaneous layer and (e) connective tissue in control animals. The tissues show normal histology in terms of cellular morphology and arrangement. Polynuclear multilobed neutrophils, fibroblast tissue and monocytes are absent in treated groups viz. Blank PG gels, Blank TEA gels, EA PG gels, EA TEA gels and gels with nanoparticles of EA, showing absence of inflammation on administering these gel formulations.

lowering of apparent viscosities. Hence these sols and gels behave as pseudo plastic or shear thinning systems. The change in viscosity with temperature for blank C-GP sol clearly indicates a transformation from sol phase to gel phase which reaches maximum at 37 °C (Fig. 8). The apparent viscosities were high for blank gel followed by PG incorporated drug loaded gel, TEA incorporated drug loaded gel and viscosity was least for C-GP sol. Lower apparent viscosities of EA loaded and EA nanoparticles loaded gels was attributed to brittle nature of these gels due to high amount of dispersed solids. On applying shear the matrix ruptured and this effect was not reverted when shear was reduced.

The viscosities of different C-GP formulations decreased with increasing rate of shear [28]. An apparent viscosity may be obtained at any rate of shear from the slope of the tangent to the curve at the specified point. The most satisfactory representation for C-GP formulations is probably a graphic plot of the entire consistency curve. Since, however, no part of the curve is linear; we cannot express the viscosities of C-GP formulations by any single value.

3.9. In vitro release studies

The cumulative release of EA from EA loaded gels (prepared using TEA and PG) and EA nanoparticles loaded gel is shown in Fig. 9. The initial release in case of EA loaded gels was rather rapid, 85% drug was released in the first 12 h followed by a slower sustained release up to 160 h. As the C-GP matrix swells, it creates a rubbery barrier for the inner drug molecules to diffuse out of the gel. Since EA was simply dispersed in C-GP matrix using co-solvents, it required dissolution prior to diffusion from the gel matrices. In case of EA nanoparticle loaded gels, the drug has to encounter an additional barrier due to entrapment in nanoparticles and this along with hydrophobic interaction between the polymer of the nanoparticles and CS retarded release of EA from nanoparticles loaded gels thereby giving sustained release of EA over a long period of time, 20% was released in 360 h and the study was terminated as much release was not observed. Various mathematical drug release models such as zero order, first order, Hixon crowell and Higuchi were adopted to predict the nature of release of EA from the gels. Hixon crowell gave the best fit ($r^2=0.98$) for EA loaded gels whereas Higuchi model gave best fit ($r^2=0.95$) for EA nanoparticle loaded gels.

3.10. Histopathological studies

Histopathological studies confirmed the biocompatibility of prepared gel formulations. Compared to the skin tissue of control group, the tissues in treated group showed no marked difference in cellular arrangement and appearance of epidermis, hair follicles, dermis, subcutaneous fat, striated muscles and connective tissue. The day after administration of gels; there was no migration of polynuclear neutrophils in the connective tissue just below the muscular layer and in subcutaneous tissue. On the 5th day, examination of treated group tissues revealed the absence of ploynuclear neutrophils and monocytes in the connective tissue and subcutaneous region, where formulations were administered. On the 15th day from the day of administration of formulations, the sections showed no signs of inflammation or necrosis (Fig. 10) and were found normal when compared to control tissues. There was no capillary proliferation, fibroblast formation and monocyte infiltration even on the 15th day of administration which showed absence of inflammation on administering these formulations in the studied period.

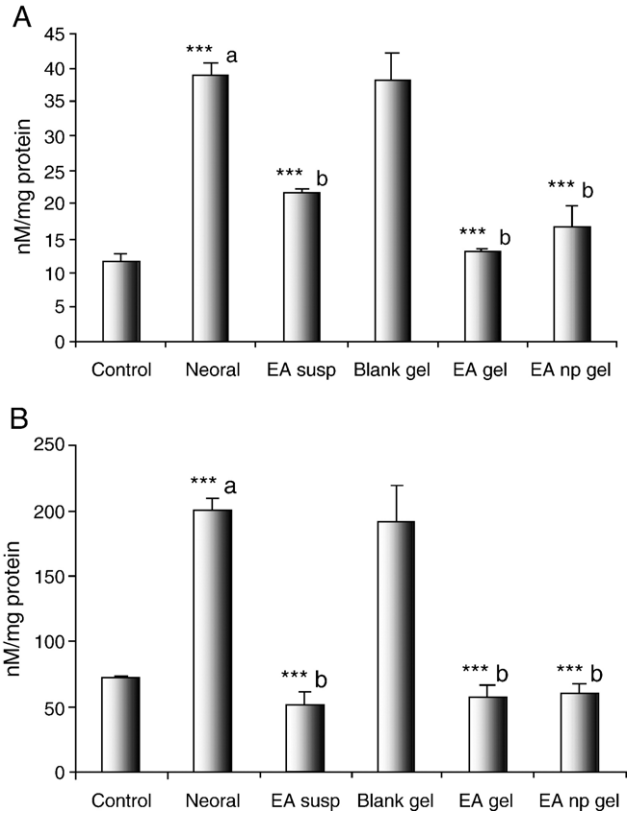

Fig. 11. Lipid peroxidation levels in different tissues measured as TBARS in different groups in CyA induced nephrotoxicity. A) Plasma and B) Kidney. Results clearly depict the effect of treatment using EA and EA nanoparticles loaded gels. Neoral: marketed CyA micro-emulsion, EA susp: EA suspension, Blank gel: blank C-GP gel, EA gel: EA loaded C-GP gel, EA np gel: EA loaded nanoparticles in C-GP gel. Values are expressed as Mean±S.E.M ($n=3$), ***$p<0.001$, a vs. control group, b vs. Neoral group.

3.11. In vivo analysis of formulations

CyA is an immunosuppressive drug widely used to prevent rejection of transplanted organs and to treat autoimmune diseases [29]. CyA therapy is often limited by adverse effects such as hypertension and nephrotoxicity mediated via ROS production [30]. CyA nephrotoxicity is characterized by renal dysfunction and by renal morphological damage with interstitial fibrosis and arteriolopathy. It has been demonstrated that CyA causes imbalance of the cellular oxidative status as a result of increased formation of free radicals [31]. Lipid peroxidation index, measured as liberation of conjugate dienes and MDA levels in kidney and plasma were used as indicators of CyA induced nephrotoxicity. Serum creatinine and BUN (blood urea

nitrogen) levels were also measured as toxicity indicators as their levels are increased in nephrotoxicity. CyA increased the production of ROS in the kidneys and this effect was accompanied by increase in MDA levels, serum creatinine levels and BUN levels as compared to control. When gel formulations containing EA and EA nanoparticles are administered, EA is directly absorbed in the systemic circulation via network of blood capillaries that surround subcutaneous tissue underneath. The sustained release of EA from gel formulations maintains required therapeutic concentrations of EA in the blood which exerts antioxidant action against CyA induced nephrotoxicity, mediated via production of free radicals in the kidney. The dose of EA administered via gel formulations was 50 mg/kg body weight for EA loaded gels and 1 mg for EA nanoparticles loaded formulations, administered every 10th day. Both the gel formulations exerted similar therapeutic response when compared to the oral formulation of EA at a much lower dose causing significant reduction in MDA levels, both in plasma and kidney (Fig. 11) and reduction in plasma creatinine and plasma BUN levels (Fig. 12). The EA C-GP gels (group 5) were capable of reverting CyA induced nephrotoxicity at a dose, 10 times lower than the dose administered in oral suspension of EA, whereas EA np C-GP gel formulations (group 6) showed similar activity at a dose, 150 times lower than the dose given orally. This study revealed that formulating nanoparticles of EA

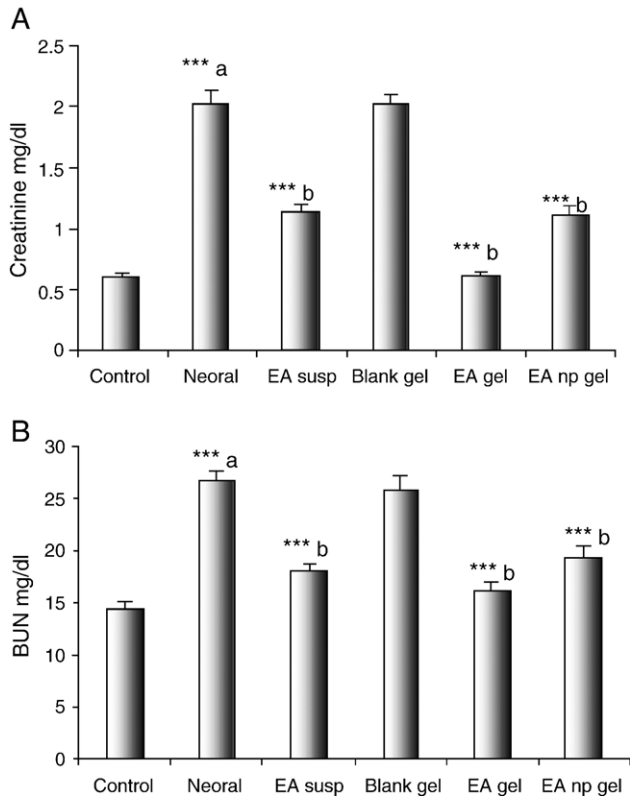

Fig. 12. Nephrotoxicity indicators in CyA induced nephrotoxicity. A) Plasma creatinine levels. B) BUN levels. Results depict the effect of treatment using EA and EA nanoparticles loaded gels. Neoral: marketed CyA micro-emulsion, EA susp: EA suspension, Blank gel: blank C-GP gel, EA gel: EA loaded C-GP gel, EA np gel: EA loaded nanoparticles in C-GP gel. Values are expressed as Mean ±S.E.M ($n=3$), ***$p<0.001$, **$p<0.01$, a vs. control group, b vs. Neoral group.

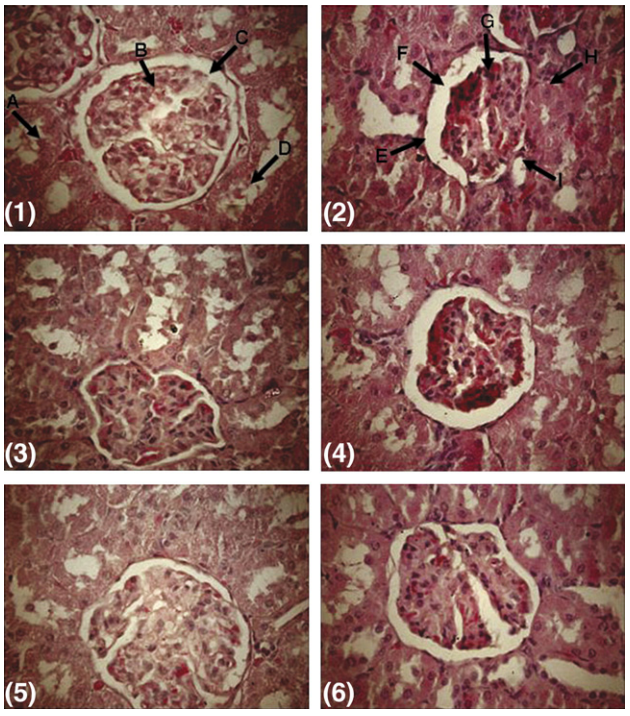

Fig. 13. Microscopic sections (hematoxylin and eosin stained) of rat kidney. (1) Control (group 1) showing normal nephron, the structural and functional unit of the kidney in the cortex region; (A) distal convoluted tubule (B) normal glomeruli showing afferent and efferent blood vessels, (C) basal membrane of nephron and (D) normal proximal convoluted tubule. The structures are normal in terms of morphology and cellular arrangement. (2) Only Neoral (group 2), treated group showing histopathological changes; (E) periglomerular fibrosis, (F) thickening of the basal membrane, (G) deposition of proteinaceous material in the glomeruli and tubules, (H) proximal tubular collapse showing flattening of tubule epithelial cells with patchy tubular necrosis, (I) non-isometric vacuolation in the proximal convoluted tubule. (3) Neoral and EA oral suspension treated (group 3). (4) Neoral and blank C-GP gel treated (group 4). (5) Neoral and EA loaded C-GP gel treated (group 5). (6) Neoral and EA np C-GP gel treated (group 6). Magnification (100×/450×/630×).

and entrapping the same in the gel manifested 15 times dose reduction when compared to gel formulations containing free EA. This demonstrates the ability of nanoparticles loaded formulation to deliver EA in a sustained manner.

Histopathology of kidneys revealed that groups 2 (only Neoral dosing) and 4 (blank gels formulations along with Neoral dosing) developed prominent histopathological changes in comparison to control (group 1). CyA caused different degree of vacuolation in proximal tubules, slight tubular necrosis, interstitial fibrosis with or without round cell infiltration, initiation of periglomerular fibrosis with mild focal capillary congestion, thickening of basal membrane and marked flattening of tubule epithelial cells which were filled with pink proteniaceous material on staining with hematoxylin and eosin and tubular collapse, with respect to untreated animals (Fig. 13). Tubular collapse and interstitial fibrosis caused alteration in kidney function which was manifested by reduction in creatinine clearing and BUN clearing capacity of the kidney and this was in agreement with biochemical tests performed earlier (refer to Fig. 13). Whereas on the other hand, treatment with EA causes marked reduction in progression of free radical mediated kidney

degeneration. Control group displayed normal kidney histology whereas groups 3, 5 and 6 showed mild to moderate focal changes which were limited to the kidney interstitium and did not affect the glomeruli and tubules both in cellular architecture and function, indicating that treatment with EA inhibits the free radical mediated damage induced by CyA. The study indicates that development and progression of CyA mediated free radical toxicity that can be ameliorated by concurrent treatment with antioxidants like EA.

4. Conclusions

The results presented in this work indicate the potential of C-GP *in situ* gelling system in improving the bioavailability of Ellagic acid. The system gels at 37 °C, has pseudoplastic character with good textural properties which affords good syringbility to the system. The system shows sustained release of ellagic acid as demonstrated by the *in vitro* release profile and the release can be further sustained by formulating nanoparticles of ellagic acid and entrapping the same in the C-GP system. Such a formulation would be best suited for sustained release of EA exhibiting improved ROS scavenging activity, as observed in the cyclosporine nephrotoxicity studies along with biocompatibility as indicated by histopathological analysis.

Acknowledgement

G.S, J.L.I, and K.S acknowledge the NIPER Fellowships (2004–2006). Start-up funds from NIPER to M.N.V.R. K. are gratefully acknowledged.

References

[1] J.M. Mates, F.M.S. Jimenez, Role of reactive oxygen species in apoptosis: implications for cancer therapy, Int. J. Biochem. Cell Biol. 32 (2000) 157–170.
[2] R.J. Mehlhorn, G. Cole, The free radical theory of aging: a critical review, Adv. Free Radic. Biol. 1 (1985) 165–223.
[3] A.Y. Sun, Y. Chen, Oxidative stress and neurodegenerative disorders, J. Biomed. Sci. 5 (1998) 401–414.
[4] H.D. Scheibmeir, K. Christensen, S.H. Whitaker, J. Jagaethesan, R. Clancy, et al., A review of free radicals and antioxidants for critical care nurses, Intensive Crit. Care Nurs. 21 (2005) 24–28.
[5] H. Sies, Free radicals in human diseases, Am. J. Med. 91 (1991) 31–38.
[6] H. Sies, Physiological role of free radicals, Exp. Physiol. 82 (1997) 291–295.
[7] B. Halliwell, J.M.C. Gutteridge, The definition and measurement of antioxidants in biological systems, Free Radic. Biol. Med. 18 (1995) 125–126.
[8] I.S. Young, J.V. Woodside, Antioxidants in health and disease, J. Clin. Pathol. 54 (2001) 176–186.
[9] B. Halliwell, Free radicals, antioxidants, and human disease: curiosity, cause or consequence? Lancet 344 (1994) 721–724.
[10] B. Halliwell, Antioxidants: the basics—what they are and how to evaluate them, Adv. Pharmacol. 38 (1997) 3–20.
[11] E. Shohami, E.B. Yannai, M. Horowitz, R. Kohen, Oxidative stress in closed heart injury: brain antioxidant capacity as an indicator of functional outcome, J. Cereb. Blood Flow Metab. 17 (1997) 1007–1019.
[12] D.V. Ratnam, D.D. Ankola, D.K. Sahana, V. Bhardwaj, M.N.V.R. Kumar, Role of antioxidants in prophylaxis and therapy: a pharmaceutical perspective, J. Control. Release 113 (2006) 189–197.
[13] K.J. Anderson, S.S. Teuber, A. Gobeille, P. Cremin, A.L. Waterhouse, F.M. Steinberg, Walnut polyphenolics inhibit in vitro human plasma and LDL oxidation, J. Nutr. 131 (2001) 2837–2842.
[14] D. Bagchi, E.A. Hassoun, M. Bagchi, S.J. Stohs, Protective effects of antioxidants against endrin induced hepatic lipid peroxidation, DNA damage, and excretion of urinary lipid metabolites, Free Radic. Biol. Med. 15 (1993) 217–222.
[15] R.C. Smart, M.T. Huang, R.L. Chang, Disposition of natural occurring antimutagenic plant phenol, ellagic acid, and its synthetic derivatives, 3-o-decylellagic acid and 3,3-di-o-methyl ellagic acid in mice, Carcinogenesis 7 (1986) 1663–1667.
[16] F. Lei, D. Xing, L. Xiang, Y. Zhao, W. Wang, et al., Pharmacokinetic study of ellagic acid in rat after oral administration of pomegranate leaf extract, J. Chromatogr., B, Biomed. Sci. Appl. 796 (2003) 189–194.
[17] N.P. Seeram, R. Lee, D. Heber, Bioavailability of ellagic acid in human plasma after consumption of ellagitannins from pomegranate (*Pubica granatum* L.) juice, Clin. Chim. Acta 348 (2004) 63–68.
[18] I. Bala, V. Bhardwaj, S. Hariharan, M.N.V.R. Kumar, Analytical methods for assay of ellagic acid and its solubility studies, J. Pharm. Biomed. Anal. 40 (2006) 206–210.
[19] A. Hatefi, B. Amsden, Biodegradable injectable in situ forming drug delivery systems, J. Control. Release 80 (2002) 9–28.
[20] M.N.V.R. Kumar, R.A.A. Muzzarelli, C. Muzzarelli, H. Sashiwa, A.J. Domb, Chitosan chemistry and pharmaceutical perspectives, Chem. Rev. 104 (2004) 6017–6084.
[21] A. Chenite, C. Chaput, D. Wang, C. Combes, M.D. Buschmann, C.D. Hoemann, J.C. Leroux, B.L. Atkinson, F. Binette, A. Selmani, Novel injectable neutral solutions of Chitosan form biodegradable gels *in situ*, Biomaterials 21 (2000) 2155–2161.
[22] I. Bala, V. Bhardwaj, S. Hariharan, J. Sitterberg, U. Bakowsky, M.N.V.R. Kumar, Design of biodegradable nanoparticles: a novel approach to encapsulating poorly soluble phytochemical ellagic acid, Nanotechnology 16 (2005) 2819–2822.
[23] I. Bala, V. Bhardwaj, S. Hariharan, S. Karade, N. Roy, M.N.V.R. Kumar, Sustained release nanoparticulate formulation containing antioxidant ellagic acid as potential prophylaxis system for oral administration, J. Drug Target. 14 (2006) 27–34.
[24] M.N. Khalid, F. Agnely, N. Yagoubi, J.L. Grossiord, G. Couarraze, Water state characterization, swelling behavior, thermal and mechanical properties of Chitosan based networks, Eur. J. Pharm. Sci. 15 (2002) 425–432.
[25] D.S. Jones, A.D. Woolfson, J. Djokic, Texture profile analysis of bioadhesive polymeric semisolids: mechanical characterization and investigation of interactions between formulation components, J. Appl. Polym. Sci. 61 (1996) 2229–2234.
[26] D.S. Jones, D.A. Woolfson, A.F. Brown, Textural, viscoelastic and mucoadhesive properties of pharmaceutical gels composed of cellulose polymers, Int. J. Pharm. 151 (1997) 223–233.
[27] N.E. Waters, The indentation of thin rubber sheets by spherical indentor, Br. J. Appl. Phys. 16 (1965) 557–563.
[28] R.E. Gariepy, A. Chenite, C. Chaput, S. Guirguis, J.C. Leroux, Characterization of thermosensitive Chitosan gels for the sustained delivery of drugs, Int. J. Pharm. 203 (2000) 89–98.
[29] J.L. Italia, V. Bhardwaj, M.N.V. Ravi Kumar, Disease, destination, dose and delivery aspects of cyclosporine: the state of the art, Drug Discov. Today 11 (2006) 846–854.
[30] S.S. Ahmed, H.W. Strobel, K.L. Napoli, J. Grevel, Adrenochrome reaction implicates oxygen radicals in metabolism of cyclosporine A and FK-506 in rat and human liver microsomes, J. Pharmacol. Exp. Ther. 265 (1993) 1047–1054.
[31] E.L. Greene, M.S. Paller, Oxygen free radicals in acute renal failure, Miner. Electrolyte Metab. 17 (1991) 124–132.